Load Modeling and Identification Based on Ant Colony Algorithms for EV Charging Stations

Shaobing Yang, Mingli Wu, Xiu Yao, *Student Member, IEEE*, and Jiuchun Jiang, *Senior Member, IEEE*

***Abstract*—Charging load modeling for electric vehicles (EVs) is a challenge due to its complexity. However, it serves as a foundation for related studies such as the impact assessment of EV charging behaviors on power system and power demand side management for EVs. The decisive factors affecting charging load profile include the power curve, the duration, and the start time of each charging process. This paper introduces the charging traffic flow (CTF) as a discrete sequence to describe charging start events, where CTF contains both spatial and temporal properties of a charging load. A set of equations are proposed to build a probabilistic load model, followed by simulation iteration steps using a flow chart. The parameter identification method based on ant colony (AC) algorithms is then studied in depth, and the pheromone update and the state transition probability are used to implement route finding and city selection, respectively. Finally, an actual case of battery swapping station is applied to verify the proposed model in both identification and simulation. The results show that the model has satisfactory accuracy and applicability.**

***Index Terms*—Ant colony algorithms, charging station, electric vehicles, load model.**

I. Introduction

NOWADAYS, electric vehicle (EV) industries are rapidly developing. The large-scale application of EVs will come soon with improvements of power battery technologies. Thus, related research topics have been receiving great attention, whose spectrum includes impact analysis of EVs on a power system, power demand side management (PDSM) for EV charging load, and economic operation optimization of a micro grid involving EVs. In particular, modeling of EV charging loads becomes very important since it is a fundamental work to support the above studies.

There are three charging modes for EVs: normal/slow, quick, and swap. The charging load in the last two modes has the following characteristics: 1) higher superposition power values; 2) larger peak-valley differentials; 3) much more difficult to shift peak loads because the waiting time greatly affects the quality of charging service. Therefore, the load of a charging station will cause significant impacts on a power distribution network [1], [2]. It is necessary to assess these impacts. For this purpose, a highly resolved load model will be very helpful, as it can directly support power flow calculation involving EVs [3], [4].

Generally, there are two traditional approaches in power load modeling: the component-based statistical synthesis and the measurement-based identification. For EV charging load, the former could have three steps: First, classify EVs as different groups according to the uses. Second, analyze the operational pattern and the proportion for each group. Last, forecast the total charging load. This approach was widely used for charging load forecasting [5]–[16]. In most studies, the distribution of charging start time was considered a crucial factor for EV charging load profile. In [5], it was analyzed based on the four charging scenarios. In [6]–[8], the EV plug-in time was represented by the normal distribution. In [9], it was obtained from the actual traffic flow measurement. In [10], it was controlled by the charging strategies. In [11] and [12], it was simulated based on the vehicle mobility patterns. In [13]–[15], it was assumed with the actual conditions. In [16], it was estimated with the arrival time distribution of an EV. Thus, many different ways are presented to describe the EV plug-in time. Although charging load profiles can be simulated with these ways, its accuracy still depends on certain assumptions or the given scenarios.

For the latter approach, the charging load model is built with unknown parameters. These parameters need to be identified based on actual measurement. In [17], an aggregation model was proposed, and the curve-fitting method was directly applied for parameter identification. However, its applicability is seriously limited because EV load profiles are significantly different from each other. In [18], a novel way was proposed to identify the number of charging EVs for the nationwide power system. However, it did not consider the charging progress dependency and the spatial feature of traffic flow.

Therefore, it is necessary to establish a generic EV charging load model with both spatial and time properties. This task has two key issues: how to describe charging start time with a universal parameter, and how to identify the parameter with an efficient algorithm based on measured data.

This paper aims to provide a more general and applicable way to describe the charging load profile and build a highly resolved probabilistic model. First, three decisive factors are analyzed individually. These are the start time, the charging power profile, and the duration of a charging process. Then, a simulation approach and its steps are presented based on the EV charging traffic flow (**CTF**). For CTF identification, suitable ant colony (AC) algorithms are selected and designed. An actual case is then studied for the validation.

Manuscript received March 11, 2014; revised July 03, 2014; accepted August 10, 2014. Date of publication September 01, 2014; date of current version June 16, 2015. This work was supported by the Fundamental Research Funds for the Central Universities (2013JBM017). Paper no. TPWRS-00353-2014.

S. Yang, M. Wu, and J. Jiang are with Beijing Jiaotong University, Beijing 100044, China (e-mail: shbyang@bjtu.edu.cn; mlwu@bjtu.edu.cn; jcjiang@bjtu.edu.cn).

X. Yao is with The Ohio State University, Columbus, OH 43210 USA (e-mail: yao.110@osu.edu).

Color versions of one or more of the figures in this paper are available online at http://ieeexplore.ieee.org.

Digital Object Identifier 10.1109/TPWRS.2014.2352263

II. Decisive Factors of Charging Load

A. Charging Start Time

The distribution of the charging start time greatly affects the load profile of a charging station. It is decided by the CTF which indicates the number of EVs coming for charging services in a fixed interval. Generally, CTF has three major factors: location, charging price, and day type. The day type, including weekday, weekend, and holiday, is the crucial factor since the location is fixed and the price is rarely changing.

In transportation field, the prediction of urban traffic flow is a very important research subject, and the day type is a decisive condition for classification. Thus, CTF can be obtained from the results of traffic activity studies. Also, it can be classified with day types. Because CTF directly contains both spatial and temporal dimensions, it brings many benefits for the charging load forecasting, especially in the case of large-scale application of EVs. More importantly, many advanced research methods in the transportation field can be used to study EV charging issues.

Define Δt as the interval in minutes, then the CTF of a day can be divided into an integer array. It can be written in the following form:

$$\{a_m\}, \quad m \in [1, L] \tag{1}$$

where m is the index of the array, a_{m} is the EV number entering the charging station during the time segment $[m-1, m]$, and L is the length of the array.

B. Charging Power Profile

A typical charging process of power batteries is shown in Fig. 1, and it has two charging stages: constant-current and constant-voltage. The power curve can be divided into multiple segments with the interval Δt. The average power values of all segments are saved into a real array. In addition, during the stage of constant-current, the charging power maintains a relative constant value. Thus, the charging power can be described by the following equation:

$$f_p(t) = \begin{cases} p_c[0], & (t > T_c) \\ p_c[T_c - t], & (t \le T_c) \end{cases} \tag{2}$$

where p_{c} is the real array which stores the discrete average power values, t is an integer to indicate the remaining charging time as $t\Delta t$, and T_{c} is an integer to indicate the length of measured power curve as $T_{\mathrm{c}}\Delta t$.

C. Charging Durations

In most cases, charging durations are different from each other in length. The charging duration of a battery is determined by the initial state of charge (SOC). For most EV drivers, the decision for charging is mainly up to the instruction from the SOC indicator. According to the law of large numbers and the central limit theorem, charging durations approximately obey a normal distribution in a large sample space. Therefore, a normally distributed random variable can be used to describe charging durations. It is written in the following form:

$$R_d \sim N_{\mathrm{Gauss}}(\mu, \sigma^2) \tag{3}$$

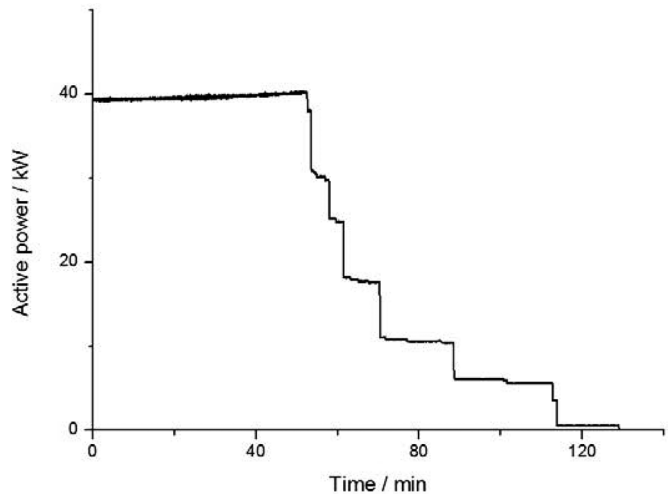

Fig. 1. Curve of active power of a charger.

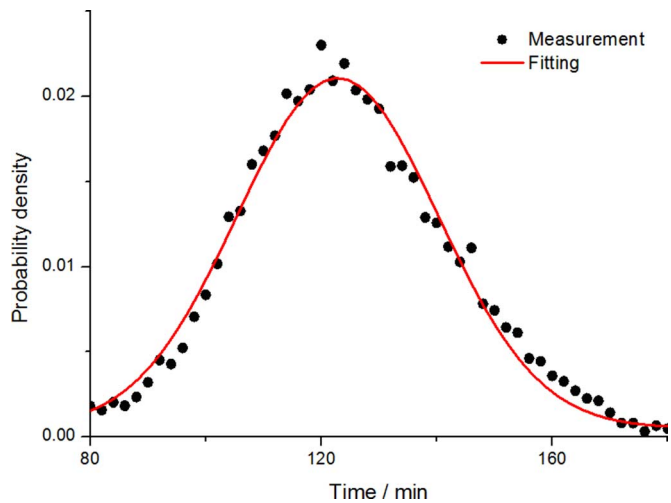

Fig. 2. Scatters of probability density of charging duration of batteries.

where N_{Gauss} is a normal distribution function, and its mean value and standard deviation are μ and σ, respectively.

The probability density shown in Fig. 2 with scatters is based on 4000 charging processes of electric buses recorded by the charging management system of the battery swapping station for the Beijing Olympic Games. The nonlinear curve-fitting is applied with (3), and the fitting result is shown by a solid line. The determination coefficient, also called R-Square, indicates the fitting degree, which is 0.985. The mean value and the standard deviation equal 123 and 17 min, respectively. Thus, (3) is considered a satisfactory way to describe the statistical features of charging durations.

III. Simulation Approach of Charging Load

According to (1)–(3), a probabilistic model can be built for the EV charging load simulation. Its simulation steps are shown in Fig. 3. In most cases, the charging power profile of the chargers is already a known condition, and the distribution of charging durations can be obtained based on historical data. Therefore, this model can be used in two ways. First, forecast or estimate the CTF of an EV charging station, then simulate

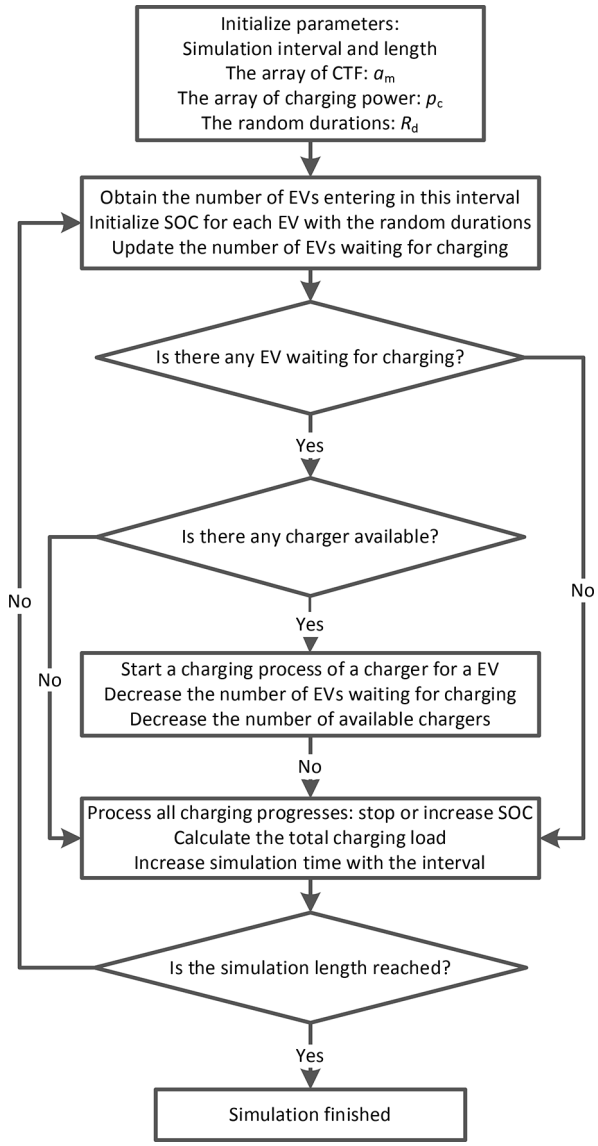

Fig. 3. Flow chart of charging load simulation.

its charging load. Second, based on testing data, identify the CTF and then build a load model. The former can be used for charging station planning, and the latter can be used for load modeling of a built station.

The proposed probabilistic model has the following features:

1) The model has a good applicability since it combines the major factors affecting charging load profiles.
2) The CTF is related to the location of a charging station and the type of day. Thus, the model can represent the influences of both space and time.
3) The model can be implemented based on the previous studies in transportation field. Thus, a universal and convincing interface is expected which will be very helpful for charging load simulation of large-scale EV applications.

For a probabilistic model, the random variable such as (3) will make the parameter identification extremely difficult. Thus, the mean value of charging durations is used for the identification instead of the random variable, and the CTF result will be considered accurate enough since a normally distributed random

TABLE I
ARRAY FOR THE CHARGING POWER CURVE
($\mu = 123$ MIN, $\Delta t = 10$ MIN)

Time range min	Average power kW	Time range min	Average power kW
[1, 10]	39.291	[71, 80]	18.874
[11, 20]	39.382	[81, 90]	10.978
[21, 30]	39.500	[91, 100]	9.855
[31, 40]	39.641	[101, 110]	6.067
[41, 50]	39.805	[111, 120]	5.642
[51, 60]	40.038	[121, 130]	2.209
[61, 70]	32.463	-	-

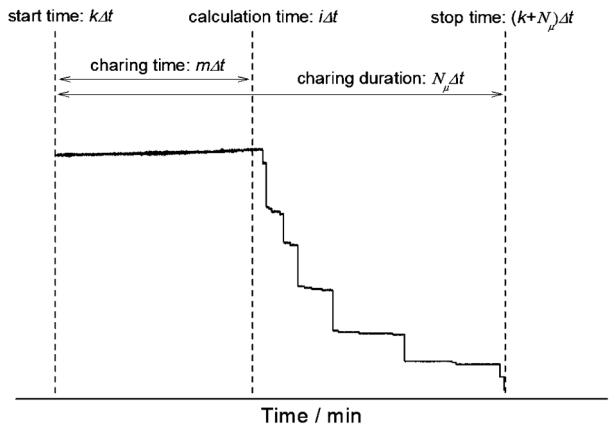

Fig. 4. Definition diagram of (4)

variable has a stable expectation. The mean length is also divided into a certain number of segments with interval Δt. According to (2), a real array is obtained to describe the charging power profile. A sample power array is shown in Table I.

The charging power array can be expressed as

$$\{v_m\}, \quad m \in [1, N_\mu] \tag{4}$$

where m is the index which indicates the charging progress, and N_μ is the array length for the mean value of charging durations.

The charging load at a given time is the sum of all charging processes that are started within the previous charging duration. According to (1) and (4), a rapid computation formula is proposed in the following form:

$$p_\Sigma(i) = \sum_{m=1}^{N_\mu} [a_{i-m} \cdot v_m] \tag{5}$$

where i represents the given calculation time, m is the charging progress, and their definitions are also shown in Fig. 4.

With (5), both the simulation and the identification can be greatly simplified and improved.

IV. IDENTIFICATION DESIGN WITH AC ALGORITHMS

A. Resolution Space Analysis

The size of resolution space is determined by the number and the range of CTF elements. According to (1), L will reach 144 if Δt is set as 10 min. If the value of the CTF elements is in the range of [0, 6], the size of the resolution space will reach 7^{144};

$$\begin{array}{cccc} v_{1K} & v_{2K} & \cdots & v_{LK} \\ \cdots & \cdots & \cdots & \cdots \\ v_{11} & v_{21} & \cdots & v_{L1} \\ v_{10} & v_{20} & \cdots & v_{L0} \end{array}$$

Fig. 5. Grid diagram of resolution space.

thus an optimization algorithm shall be selected in searching for a global optimal solution. More importantly, CTF elements must be simultaneously resolved due to their correlation.

Most optimization algorithms such as genetic algorithms (GAs) and simulated annealing algorithms (SAAs), rely on the global error to establish the objective function. However, the global error is not suitable for the parameter identification case due to two major reasons: First, at a given time, the simulation error is only related to the charging start events during the previous duration instead of all events. Second, the variation of each CTF element only affects the simulated load in the next charging duration. As such, both global and local optimizations shall be achieved at the same time. The latter is especially important. Therefore, AC is the best choice for the parameter identification because its objective function can be designed with local errors. This leads to better performance in terms of convergence speed and precision.

Here, if the range of CTF elements is set as $[0, K]$, the resolution space can be defined to be a nodal grid of $L \times (K+1)$ dimensions, as shown in Fig. 5. Each node represents a city in a route for AC algorithms and its location is the intersection of the column and the row. Thus, each column corresponds to a time segment, and each row is considered as a CTF element value. For example, v_{xy} indicates that the element value equals y in the segment x. It means that y EVs enter the charging station in the segment $[x-1, x]$.

According to AC algorithms, in one iteration, each ant must accomplish a search route consisting of L nodes (cities) from the left-most column to the right-most one, and the row selection at each column for ants depends on the state transition probability.

The measured data for a charging load can be saved as a real array according to the interval Δt. The array is written in the following form:

$$\{w_i\}, \quad i \in [1, L] \tag{6}$$

where w_{i} is the total load at the time $i\Delta t$.

Once a charging process starts, the charger will reach its rating power in a very short time, such as a few minutes. Thus, the CTF element value of the segment i can be restricted by the following equation:

$$K_i = \min(\mathrm{int}(w_i/p_e), K) \tag{7}$$

where i is the column index, min is the function to return the smallest one from the given values, and p_{e} is the rated power of the charger.

According to (7), the tabu table of AC algorithm can be established, which means the size of solution space can be significantly reduced.

B. AC Operator Designs

AC algorithms have two key operators: pheromone update and city selection. The former is designed using feedback from the simulation error, and the latter is achieved with the state transition probability. Each ant needs to complete two steps when it arrives at a column: First, update its related pheromone elements according to the error caused by the row selections within the previous charging duration. Second, select a node (row) at this column according to the state transition probability.

In the procedure of parameter identification, (5) is used to simulate the charging power values for all columns. Define x as the index of a column. The simulation error is written as the following equation:

$$e_x = p_\Sigma(x) - w_x \tag{8}$$

where x is the column index.

According to (5), $p_\Sigma(x)$ is determined by multiple charging events started during the range of $[x-N_\mu, x-1]$. Thus e_{x} can be used to update the pheromone elements within this range. The updating equation is written as

$$\tau_{ij}^{\mathrm{new}} = (1-\rho)\tau_{ij}^{\mathrm{old}} + \frac{Q}{(e_x)^2 + c}, \quad (i = x - N_\mu, \ldots, x-1;\ j = a_i) \tag{9}$$

where τ is the pheromone matrix of size $L \times (K+1)$, i is the column index of each element within the range of $[x - N_\mu, x-1]$, j is the selected row index of the column i, Q is the pheromone intensity, ρ is the evaporation coefficient, and c is a very small positive real constant to prevent zero division.

Meanwhile, for the column x, the row selection depends on the state transition probability. It can be calculated by the following equation:

$$p_{xj} = \frac{[\tau_{xj}]^\alpha [\eta_{xj}]^\beta}{\sum_{i=0}^{K_x} [\tau_{xi}]^\alpha [\eta_{xi}]^\beta}, \quad (j = 0, \ldots, K_x) \tag{10}$$

where j is the selected row index of the column x, i is an integer, K_{x} is an integer obtained with (7), α is the heuristic factor of information, β is the heuristic factor of expiration, and η is the heuristic function.

With (10), the state transition probabilities of all the rows of column x can be calculated. It follows that a row can be selected according to the uniform distribution. In AC algorithms, the heuristic function plays a very important role since it can increase the local searching capability. It needs to be designed with the full effects caused by the row selection.

First, for column x, if row y is selected, the simulated load results during the index range of $[x+1, x+N_\mu]$ are all affected. Based on (5), the simulated load at this column can be obtained by the following equation:

$$p_\Sigma(i; x, y) = \sum_{\substack{m=1 \\ m \neq i-x}}^{N_\mu} [a_{i-m} \cdot v_m] + y \cdot v_{i-x}, \quad (i \in [x+1, x+N_\mu]). \tag{11}$$

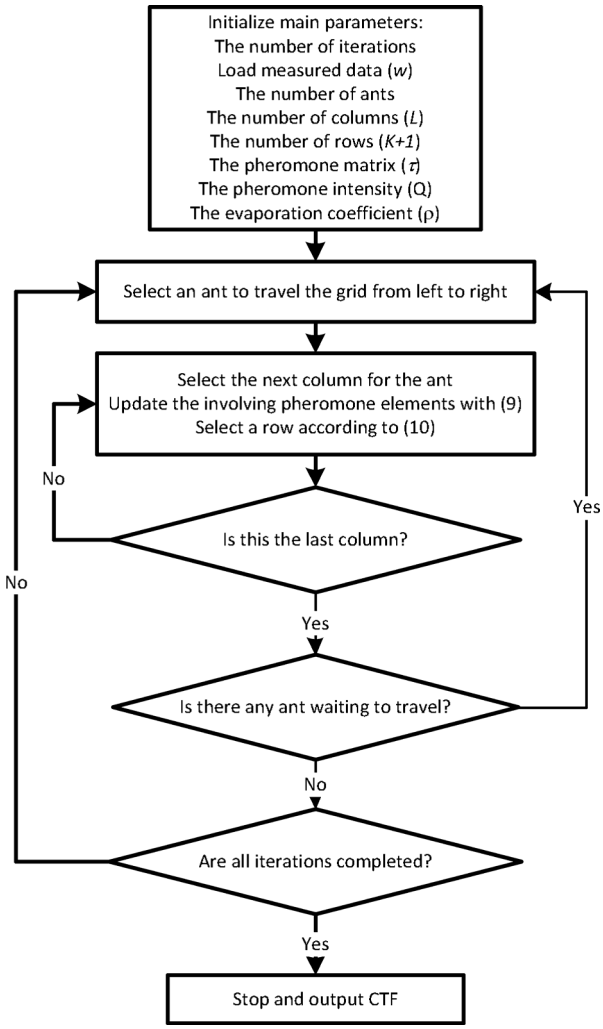

Fig. 6. Flow chart of parameter identification.

Second, the total error can be written in the following form:

$$\delta_{xy} = \frac{1}{N_\mu} \sum_{i=x+1}^{x+N_\mu} [p_\Sigma(i; x, y) - w_i]^2. \tag{12}$$

Lastly, the heuristic function can be given as the following equation:

$$\eta_{xy} = \frac{1}{\delta_{xy} + c}. \tag{13}$$

The detailed steps for the parameter identification with AC algorithms are presented in Fig. 6.

V. Case Validation

The charging station to serve electric buses for the Beijing Olympic Games is taken as an example. This station has been serving electric buses since 2008. The measured data were acquired in 2010. At that time, there were already two electric bus lines and over 30 buses supported by this charging station. These buses run 16 h per day like the regular buses. The 1-h average power values of the five Thursdays of September in 2010 are selected for CTF identification. They are shown in Fig. 7 by a histogram. The conditions are set as follows:

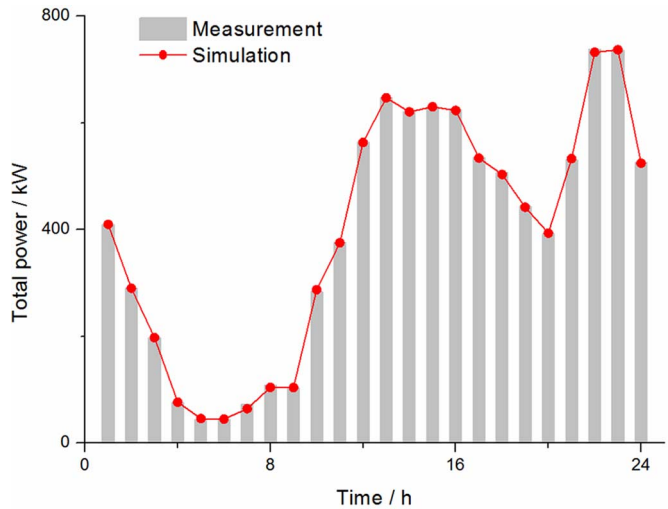

Fig. 7. Comparison with simulation to measurement of charging load.

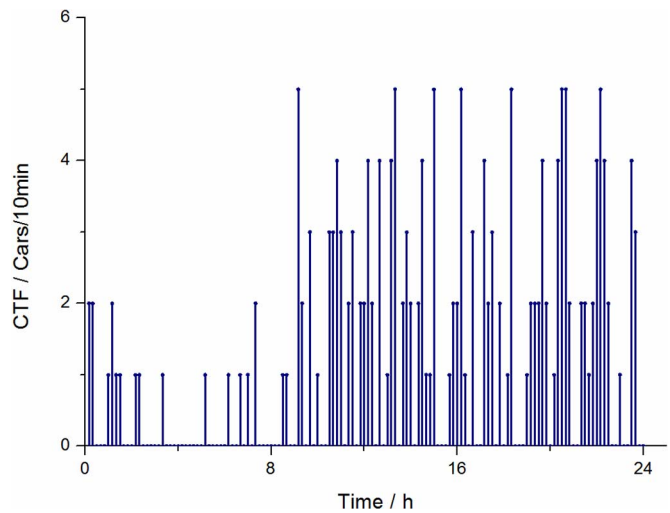

Fig. 8. CTF identification result.

1) $\Delta t = 10$ min, $N_\mu = 13$, and Table I is used to describe the charging power curve.
2) The array w is loaded with the 24 1-h power values.
3) Set $K = 6$, then row indexes are in the range of [0, 6].
4) $Q = 5000$, $\rho = 0.5$, $\alpha = 1$, $\beta = 1$, c = 1e−10, and set all values of the τ matrix to be 20.
5) Set the ant number to be 600, and set the iteration times to be 100.

The computation of charging load has a satisfying speed since (5) is based on the fundamental operations of arithmetic. The identified CTF values are shown in Fig. 8, and each one is presented as a pulse. The pulse height indicates the number of EVs entering for charging in the previous 10 min.

According to the CTF, simulation can be implemented with (5), and the results are shown with the solid dots and lines in Fig. 7. In this case, the R-Square value reaches 1.000. In addition, the errors are given in Table II. The mean absolute percentage error (MAPE) is less than 1.3%. Thus, the identification accuracy with AC is greatly satisfactory.

TABLE II
COMPARISON WITH SIMULATION TO MEASUREMENT

Hour	Measured data / kW	Simulated data / kW	Error / %	Statistical mean / kW	Error/%
1	410.0	409.7	0.0	428.1	4.4
2	289.2	296.4	0.3	300.3	3.9
3	197.5	197.6	0.1	180.3	-8.7
4	75.0	76.4	1.9	72.6	-3.2
5	44.1	45.6	3.4	44.8	1.6
6	43.3	44.8	3.5	43.6	0.8
7	72.1	64.1	-11.1	64.0	-11.3
8	108.3	104.2	-3.9	98.1	-9.4
9	102.5	102.3	1.4	105.4	2.9
10	283.3	280.6	1.4	252.6	-10.8
11	376.3	368.1	-0.2	337.3	-10.4
12	563.8	553.7	0.0	535.4	-5.0
13	647.1	649.9	0.0	635.6	-1.8
14	621.3	620.9	0.0	618.3	-0.5
15	630.0	630.7	0.1	625.0	-0.8
16	625.0	623.8	-0.2	592.7	-5.2
17	535.0	534.7	-0.1	511.9	-4.3
18	506.3	504.4	-0.6	513.5	1.4
19	443.3	446.7	-0.3	447.0	0.8
20	391.7	393.6	0.5	373.8	-4.6
21	530.4	533.8	0.5	507.2	-4.4
22	737.9	737.6	-0.7	737.1	-0.1
23	736.3	736.4	0.1	766.1	4.1
24	526.3	531.4	-0.3	549.5	4.4

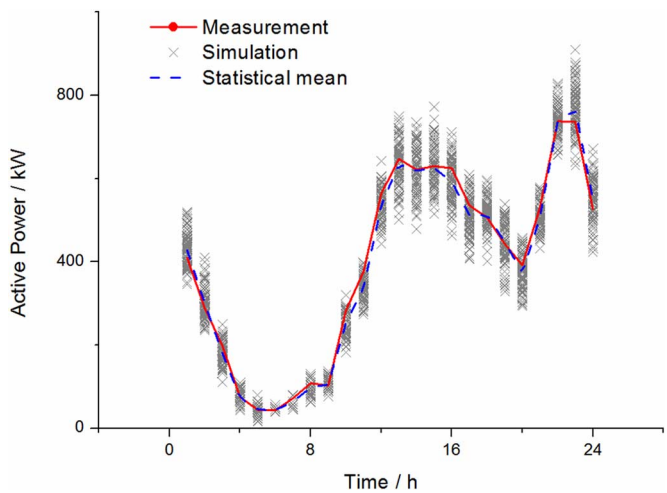

Fig. 9. Probabilistic simulation result of charging load.

Moreover, the proposed model can be used to produce probabilistic results with Monte Carlo method. According to (3), set μ and σ as 123 and 17 min, respectively. Then, pseudo-random numbers can be produced as the charging durations. Based on Fig. 3, a computer program has been built for simulation. The 1-h power values for 100 Thursday samples are produced and shown in Fig. 9 with crosses. The statistical mean values are also presented with a dash line.

Although the charging duration fluctuates significantly, the charging load profile still presents a clear and stable feature. At each hour, the power values have an expectation which is very close to the real one. The errors of mean values are given in Table II, and its MAPE is less than 4.4%.

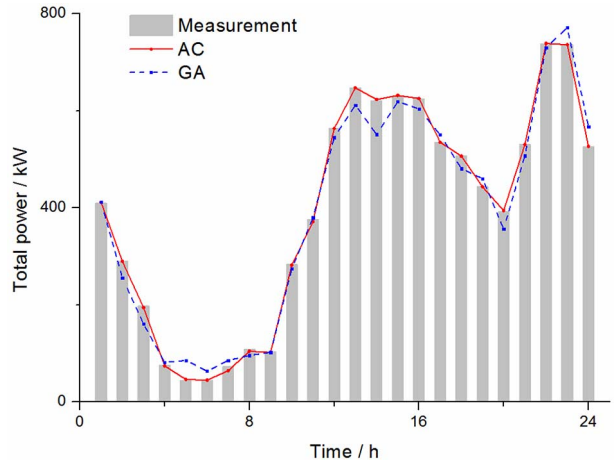

Fig. 10. Accuracy comparison with AC to GA.

TABLE III
PERFORMANCE COMPARISON WITH AC TO GA

Algorithms	Computational cost	MAPE	R-Square
AC	12 s / 100 iterations	1.3%	1.000
GA	39 s / 100 iterations	11.6%	0.985

Furthermore, a comparative analysis has been carried out to benchmark the identification approach of AC algorithms in performance. Based on the global error of charging load, a computer program with GA has been developed for CTF identification. A computer is used to run AC and GA in single-threaded mode. The software SuperPI which calculates the mathematical constant π to a specific number of decimal digits is selected to test the single-threaded computing capability of this computer. The computational cost of π up to 1 million decimal digits is about 13 s using the version 1.9 of SuperPI. The comparison result of AC and GA is presented in Table III and Fig. 10. The AC algorithm has significant advantages in accuracy and efficiency since (11)–(13) have been utilized to enhance its local searching capability.

VI. CONCLUSION

The decisive factors affecting charging load characteristics are the distribution of durations, the power profile of chargers, and the charging start time. The proposed CTF can be introduced to describe the charging start time. Furthermore, it contains the properties of both space and time.

The proposed model provides flexible modes for simulation and parameter identification. In simulation, it can be used in both stochastic and deterministic situations. In parameter identification, (5) provides a rapid calculation method to improve the efficiency.

All elements of CTF are linked one by one, and the charging power at a certain time is determined by a group of elements within the previous charging duration. Thus, the parameter identification does not entirely depend on a global error. With a particular design on the objective function, the proposed AC algorithm has shown outstanding performance in accuracy and computational efficiency.

CTF brings a new approach to the study on EV charging load profiles. To benefit from the interdisciplinary cooperation, the research results on traffic activities can be used on EV load modeling. In the future, a universal platform can be built for large-scale EV applications based on the concept of CTF.

REFERENCES

[1] J. A. P. Lopes, F. J. Soares, and P. M. R. Almeida, "Integration of electric vehicles in the electric power system," *Proc. IEEE*, vol. 99, no. 1, pp. 168–183, Jan. 2011.

[2] M. Etezadi-Amoli, K. Choma, and J. Stefani, "Rapid-charge electric-vehicle stations," *IEEE Trans. Power Del.*, vol. 25, no. 3, pp. 1883–1887, Jul. 2010.

[3] J. G. Vlachogiannis, "Probabilistic constrained load flow considering integration of wind power generation and electric vehicles," *IEEE Trans. Power Syst.*, vol. 24, no. 4, pp. 1808–1817, Nov. 2009.

[4] G. Li and X.-P. Zhang, "Modeling of plug-in hybrid electric vehicle charging demand in probabilistic power flow calculations," *IEEE Trans. Smart Grid*, vol. 3, no. 1, pp. 492–499, Mar. 2012.

[5] K. Qian, C. Zhou, M. Allan, and Y. Yuan, "Modeling of load demand due to EV battery charging in distribution systems," *IEEE Trans. Power Syst.*, vol. 26, no. 2, pp. 802–810, May 2011.

[6] Y. Cao, S. Tang, C. Li, P. Zhang, Y. Tan, Z. Zhang, and J. Li, "An optimized EV charging model considering TOU price and SOC curve," *IEEE Trans. Smart Grid*, vol. 3, no. 1, pp. 131–138, Mar. 2012.

[7] P. Papadopoulos, S. Skarvelis-Kazakos, I. Grau, L. M. Cipcigan, and N. Jenkins, "Electric vehicles' impact on British distribution networks," *IET Electr. Syst. Transp.*, vol. 2, no. 3, pp. 91–102, Apr. 2011.

[8] S. Shao, M. Pipattanasomporn, and S. Rahman, "Grid integration of electric vehicles and demand response with customer choice," *IEEE Trans. Smart Grid*, vol. 3, no. 1, pp. 543–550, Mar. 2012.

[9] Y. Zheng, Z. Y. Dong, Y. Xu, K. Meng, J. H. Zhao, and J. Qiu, "Electric vehicle battery charging/swap stations in distribution systems: Comparison study and optimal planning," *IEEE Trans. Power Syst.*, vol. 29, no. 1, pp. 221–229, Jan. 2012.

[10] J. Lassila, V. Tikka, J. Haakana, and J. Partanen, "Electric cars as part of electricity distribution—Who pays, who benefits?," *IET Electr. Syst. Transp.*, vol. 2, no. 4, pp. 186–194, Feb. 2012.

[11] P. Sánchez-Martín, G. Sánchez, and G. Morales-España, "Direct load control decision model for aggregated EV charging points," *IEEE Trans. Power Syst.*, vol. 27, no. 3, pp. 1577–1584, Aug. 2012.

[12] A. Lojowska, D. Kurowicka, G. Papaefthymiou, and L. van der Sluis, "Stochastic modeling of power demand due to EVs using copula," *IEEE Trans. Power Syst.*, vol. 27, no. 4, pp. 1960–1968, Nov. 2012.

[13] Y. Ma, T. Houghton, A. Cruden, and D. Infield, "Modeling the benefits of vehicle-to-grid technology to a power system," *IEEE Trans. Power Syst.*, vol. 27, no. 2, pp. 1012–1020, May 2012.

[14] K. Clement-Nyns, E. Haesen, and J. Driesen, "The impact of charging plug-in hybrid electric vehicles on a residential distribution grid," *IEEE Trans. Power Syst.*, vol. 25, no. 1, pp. 371–380, Feb. 2010.

[15] M. A. Ortega-Vazquez, F. Bouffard, and V. Silva, "Electric vehicle aggregator/system operator coordination for charging scheduling and services procurement," *IEEE Trans. Power Syst.*, to be published.

[16] S. Huang and D. Infield, "The impact of domestic plug-in hybrid electric vehicles on power distribution system loads," in *Proc. Int. Conf. Power Syst. Technol.*, Oct. 2010.

[17] J. Zheng, X. Wang, K. Men, C. Zhu, and S. Zhu, "Aggregation model-based optimization for electric vehicle charging strategy," *IEEE Trans. Smart Grid*, vol. 4, no. 2, pp. 131–138, Jun. 2013.

[18] P. Zhang, K. Qian, C. Zhou, B. G. Stewart, and D. M. Hepburn, "A methodology for optimization of power systems demand due to electric vehicle charging load," *IEEE Trans. Power Syst.*, vol. 27, no. 3, pp. 1628–1636, Aug. 2012.

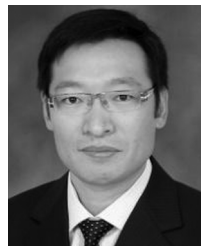

Shaobing Yang received the B.S. degree from Shanghai Jiaotong University, Shanghai, China, in 1995 and the M.S. degree from Beijing Jiaotong University, Beijing, China, in 2009, both in electrical engineering.

He is an Associate Professor of the School of Electrical Engineering in Beijing Jiaotong University. His research interests include power system simulation, load modeling, demand side management, electric power quality, and load forecasting for electric vehicles.

Mingli Wu received the B.S. and M.S. degrees in electrical engineering from Southwest Jiaotong University, Chengdu, China, in 1993 and 1996, respectively, and the Ph.D. degree in electrical engineering from Beijing Jiaotong University, Beijing, China, in 2006.

He is a Professor of the School of Electrical Engineering in Beijing Jiaotong University. His current research areas include power supply for electric railways, digital simulation of power systems, and electric power quality.

Xiu Yao (S'10) received the B.S. and M.S. degrees from Xi'an Jiaotong University, China, in 2007 and 2010, respectively. She is currently pursuing the Ph.D. degree in The Ohio State University, Columbus, OH, USA.

Her current research interests include dc arc fault detection in high voltage and power electronic systems, harmonic elimination of multilevel inverter, and the utilization of modular multilevel converter in high power systems.

Jiuchun Jiang (M'12–SM'14) was born in Jilin Province, China. He received the B.S. degree in electrical engineering and the Ph.D. degree in power system automation from Northern Jiaotong University, Beijing, China, in 1993 and 1999, respectively.

He is currently a Professor with the School of Electrical Engineering, Beijing Jiaong University. His main interests are related to battery application technology, electric car charging stations, and micro-grid technology.

Prof. Jiang received the National Science and Technology Progress 2nd Award for his work on EV Bus system, and the Beijing Science and Technology Progress 2nd Award for his work on EV charging system.